The 2016 World Congress on
Advances in Civil, Environmental, and Materials Research (ACEM16)
Jeju Island, Korea, August 28-September 1, 2016

Passive Aerodynamic Facilities for Flutter Control and Corresponding Applicable Bridge Deck Types

*Ke Li[1)], Yaojun Ge[2)], Yongxin Yang[3)] and Jinlin Xia[4)]

[1), 2), 3), 4)] *State Key Laboratory of Disaster Reduction in Civil Engineering, Tongji University, Shanghai, China*

[1)] *keli-bridge@tongji.edu.cn*

ABSTRACT

With experience from considerable studies on the shape optimization, several aerodynamic appendages are found to be useful to increase the flutter stability of certain girder types, namely, streamlined box girder, Π shaped girder and bluff girder with cantilever. Specifically, stabilizer is found to be useful in all of the three typical girders, but adjustments on slotting and inspection rails are beneficial only in streamlined box girder and bluff box girders, respectively. Wind tunnel experiments and computational-fluid-dynamics methods are introduced to investigate their flutter control effects and corresponding mechanisms, trying to figure out a general guideline for the flutter suppression in future researches.

1. INTRODUCTION

Aero-elastic flutter is one of the most dangerous phenomenon which can lead the collapse of the whole bridge, after a period of gradually increasing oscillation of the bridge girder. This threat is especially outstanding in long-span bridges, due to the decreasing stiffness with growing spans.

Flutter attracted the attention of bridge engineers after the now iconic Tacoma Narrows bridge disaster (Billah and Scanlan 1991). Its main span collapsed into the Tacoma Narrows only four months after its construction, due to a 19m/s wind. Subsequent studies have revealed the nature of flutter as one type of dynamic instability, and have successfully avoided the reappearance of such disaster by elaborately selecting structural form and aerodynamic shape of the girder (Simiu and Scanlan 1986). The affiliated elements to change the aerodynamic shape of the girder are commonly regarded as passive control facilities, because of their independence of energy supply. Applications in practical engineering have proved their effectiveness

---

[1), 4)] Graduate Student
[2), 3)] Professor

and robustness, making possible of long-span bridges surviving from strong wind environment in projects of crossing oceans and connecting islands. Akashi Kaikyo Bridge in Japan, with a truss stiffen girder, has set the bridge span record to 1991m (Miyata 2003, Makoto 2004) with the help of central stabilizer (Fig. 1a). The 1650m span Xihoumen Bridge in China keeps the longest span box-girder in the world (Ge and Xiang, 2011), using a central slotting to ensure its flutter stability (Fig. 1b). Moreover, the planned Messina Strait Bridge with a central span of 3300m (Brown 1996) also introduces the slotting method to meet the local design wind speed (Fig. 1c).

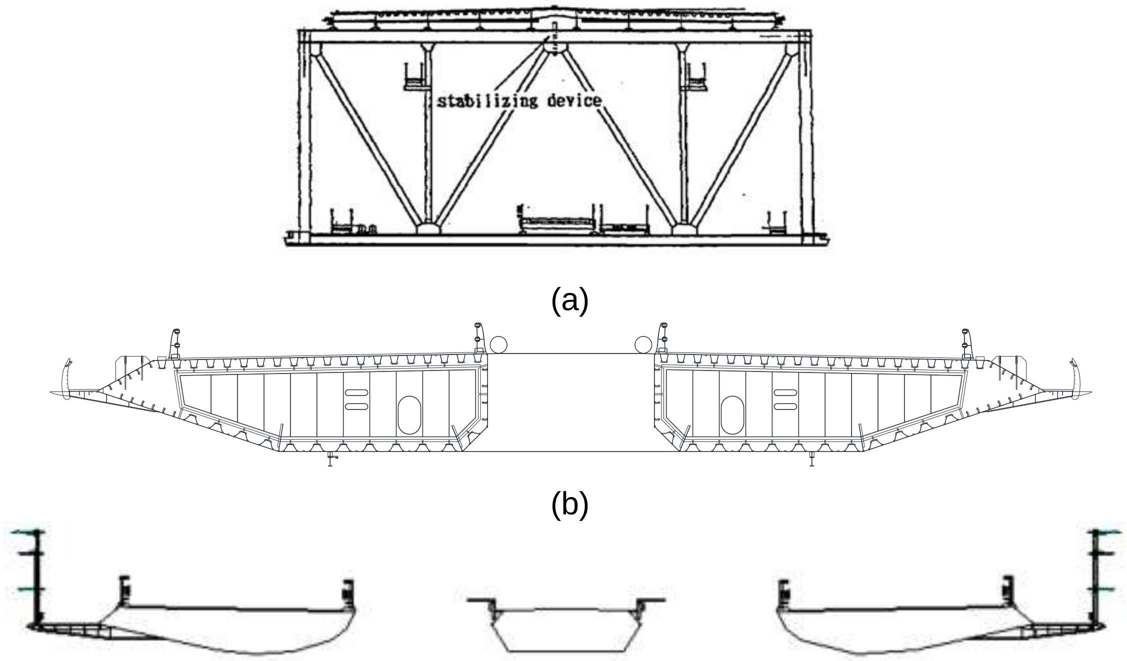

(a)

(b)

(c)

Fig. 1 Applications of passive control facilities. (a) Central stabilizer in Akashi Kaikyo Bridge. (b) Central slotting in Xihoumen Bridge. (c) Multi-slotting in Messina Strait Bridge.

Till now, passive aerodynamic facilities have become the most widely used method to suppress the flutter of long-span bridges, and on which numerous studies have been carried out all over the world. Among these efforts, our research team has also accumulated much experience about the aerodynamic shape optimization and corresponding control mechanisms.

In this paper, several passive control facilities are discussed, categorized according to their most applicable bridge deck types (Fig. 2). To be specifically, wind tunnel tests for streamlined box girder, bluff girder with cantilever and Π shaped girder are given in the first part, respectively. In this part, the positions, sizes or shapes of the facilities are adjusted, and the control effect tendencies highlight the importance of shape optimization. Later, control mechanisms of the stabilizer, slotting, inspection rails and wind faring are discussed through Computational-Fluid-Dynamics (CFD) method in the second part. Phase and amplitude of the surface pressure are compared in cases with and without passive facilities. Furtherly, work of the pressure is calculated to give an overall demonstration of the influence after control.

type	useful passive aerodynamic facilities
streamlined box girder	
bluff girder with cantilever	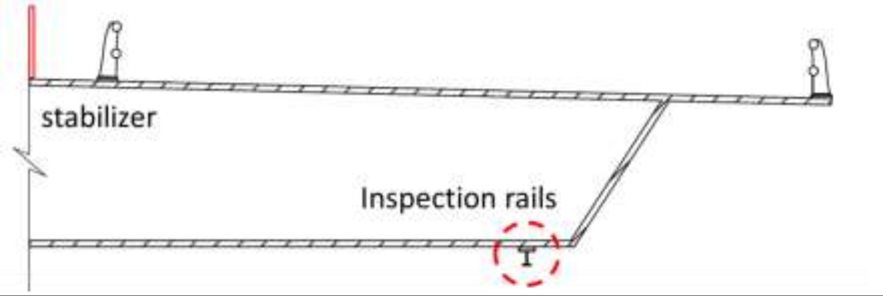
Π shaped girder	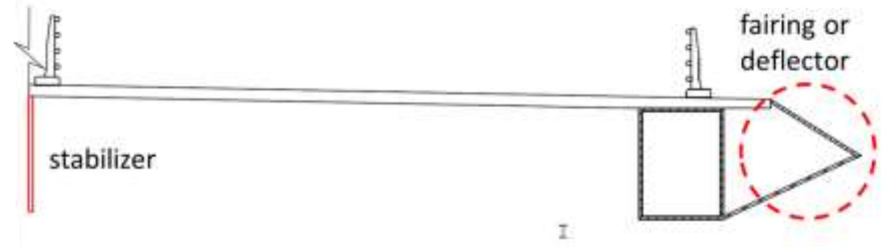

Fig. 2 Three commonly used girder type, and corresponding flutter control facilities.

2. SUGGESTED FACILITIES FOR STREAMLINED BOX GIRDER

Streamlined box girder is one of the most favorable girder type for long-span bridges. It can increase the torsional stiffness of the girder and reduce the horizontal wind load. The span record of its application without passive aerodynamic facilities is held by the 1624m Great Belt Bridge in Denmark, where the flutter critical speed is 62m/s, close to the upper limit of the closed box girder. To further improve the flutter stability, some passive aerodynamic facilities are found to be particularly useful.

2.1 Slotting

Slotting is to separate the bridge girder into several parallel pieces, which are connected to each other by cross beams. The girder can still vibrate as a whole, but air is allowed to pass through the slotting. Central slotting has been applied to the longest span box-girder bridge in the world, namely, the 1650m span Xihoumen bridge. And multiple slotting has been accepted to the planned Messina Strait Bridge, with a central span of 3300m.

In our researches, a series of wind tunnel tests have been carried out to figure out the evolution tendency between the slotting width and the flutter critical speed. The deck shape of the down scaled sectional model is given in Fig. 3, in which the slotting width (D) can be adjusted. Dynamic characteristics of the model are fixed. Mass and inertial mass are $6.72\mathrm{kg/m}$ and $0.37\mathrm{kg \cdot m^2/m}$, respectively. Frequencies of heaving mode and pitching mode are $1.34\mathrm{Hz}$ and $2.66\mathrm{Hz}$, respectively.

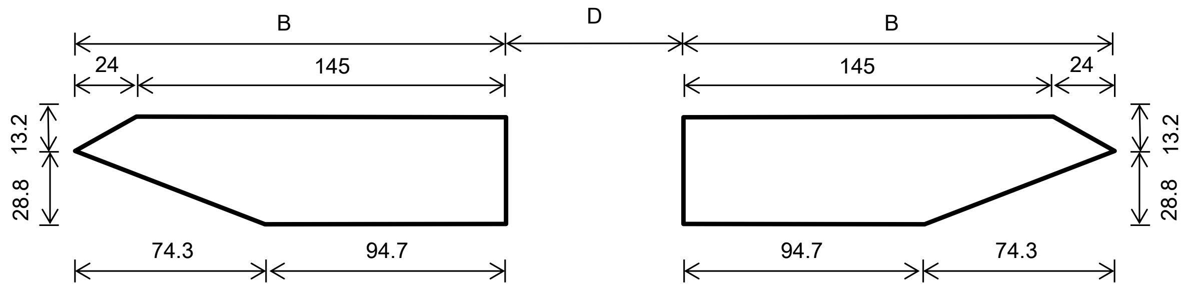

Fig. 3 Sectional model with adjustable slotting width (mm).

The flutter critical speed of the sectional model is examined with different slotting ratios (D/B) and different wind attack angles. The results are given as Tab. 1, and the control effects are compared in Fig. 4, showing the tendencies of the critical speed and also the growth rate (Zhou, 2005).

Tab. 1 Flutter critical speeds with different slotting widths.

Slotting ratio (D/B)	Flutter critical speed (m/s)			Critical case
	$+3°$	$0°$	$-3°$	
0%	14.5	15.0	16.4	$+3°$
20%	15.5	18.0	18.0	$+3°$
40%	17.5	19.8	20.2	$+3°$
60%	16.8	20.4	20.7	$+3°$
80%	15.6	19.6	20.0	$+3°$
100%	14.3	17.9	18.6	$+3°$

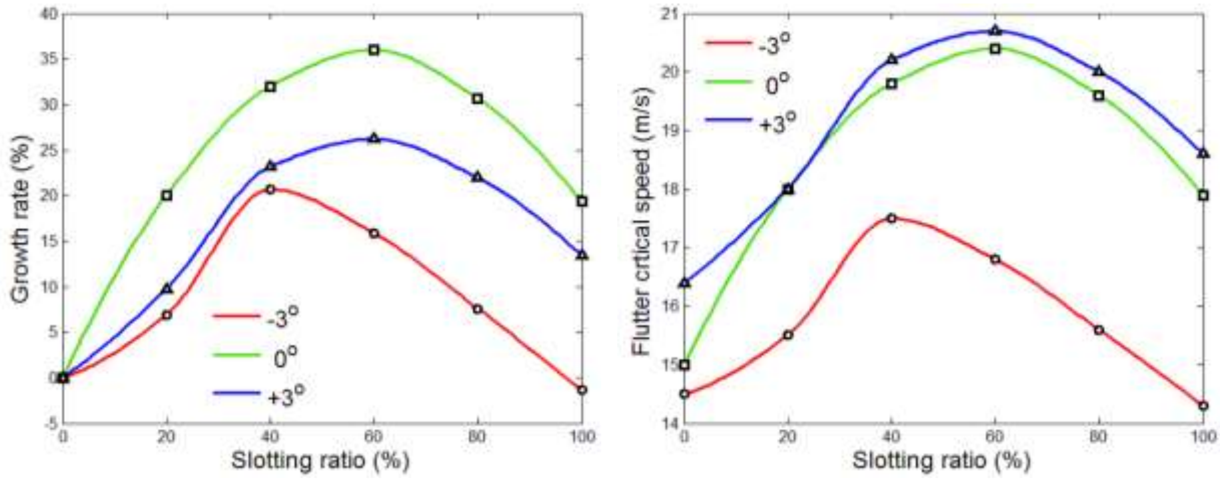

(a) (b)

Fig. 4 Control effects with different slotting widths. (a) Tendencies of flutter critical speed. (b) Tendencies of growth rate.

It can be recognized that the control effect is firstly increased and then decreased with the growing slotting width, and there exists one optimal point that the flutter critical speed reaches the maximum value. Although the flutter stability is improved most significantly with $0°$ wind attack angle (Fig. 4b), the flutter critical speed is always determined by the $+3°$ case (Fig. 4a).

2.2 Stabilizer

Stabilizer is another useful aerodynamic appendage. It has been used in the 1490m span Runyang bridge in China. To examine the control effectiveness and robustness, a series of wind tunnel tests are designed, with three types of the stabilizer, demonstrated in Fig. 5. The one with only upper stabilizer is named as X type, the one with only lower stabilizer is named as Y type, and the one with both installed is named as XY type. Mass and inertial mass are $42.9\mathrm{t/m}$ and $15204\mathrm{t\cdot m^2/m}$, respectively. Frequencies of heaving mode and pitching mode are $0.099\mathrm{Hz}$ and $0.195\mathrm{Hz}$, respectively.

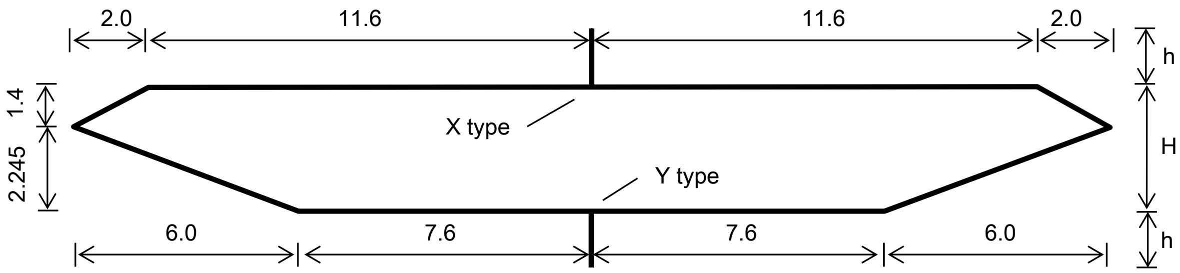

Fig. 5 Tested bridge girder with stabilizer (m).

Tab. 2 Flutter critical speeds with different slotting widths.

h/H	Flutter critical speed (m/s)								
	X type			Y type			XY type		
	+3°	0°	−3°	+3°	0°	−3°	+3°	0°	−3°
0%	87.0	90.0	98.4	87.0	90.0	98.4	87.0	90.0	96.4
20%	91.2	115.2	109.8	90.0	110.4	111.6	72.0	108.6	127.2
40%	96.0	118.8	102.0	82.8	102.0	112.8	106.2	102.0	87.0
60%	111.0	105.0	96.0	72.0	99.0	110.4	108.6	91.8	-
80%	121.2	94.8	91.2	55.8	91.2	95.4	-	-	-

Note: - is for soft flutter.

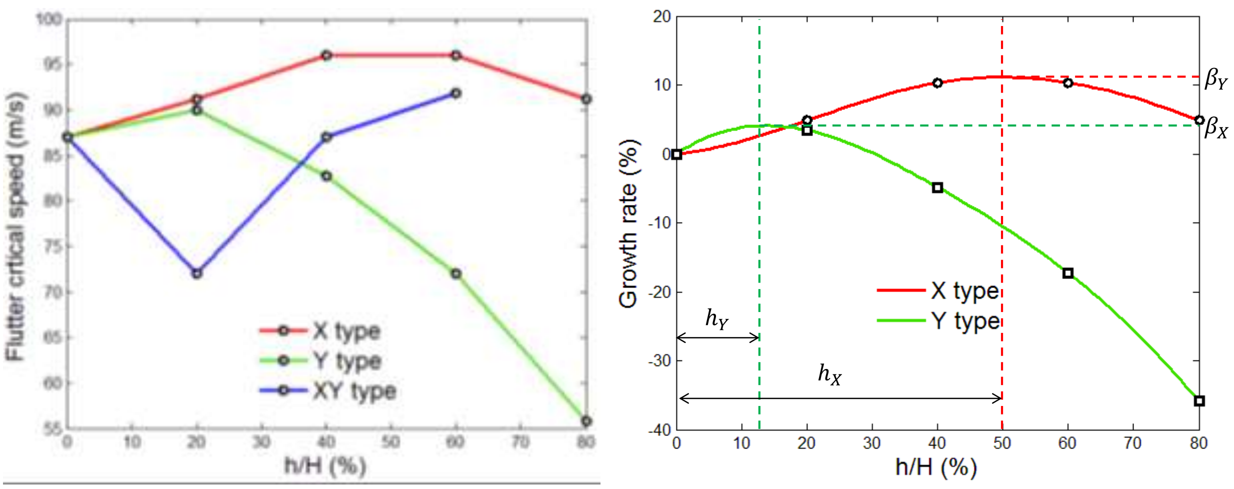

Fig. 6 Control effects with different slotting widths. (a) Tendencies of flutter critical speed. (b) Tendencies of growth rate.

The flutter critical speed with different stabilizer types are examined in cases of changing stabilizer height and also scattered wind attack angles (Yang, 2014). The results are given in Tab. 5, showing a much different phenomenon compared to the cases with changing slotting ratios. It can be recognized that the flutter critical speed with one stabilizer type does not always occurs in certain wind attack angle. Therefore, the decisive flutter critical speeds, namely the lowest one in different wind angles, are demonstrated in Fig. 6 (a). It is obvious that the X type and Y type can both increase the critical speed in a stable way, while the XY type may bring adverse effect when the plate height is low. From the growth ratio shown in Fig. 6 (b), it is obvious that upper stabilizers are more effective and robust, namely, the control effect show an increasing tendency in a wide range of plate height, and the optimal effect is better than lower stabilizers.

2.3 Wind faring

Although slotting and stabilizer is helpful for flutter, they may cause vortex-induced-vibration during service. For this reason, optimizing only the wind faring is still an attractive way (Wang, 2010). The optimizations are carried out based on a sectional model shown in Fig. 7. The height of the girder is 0.04m. Through changing the faring angle β and the dip angle α of the inclined web, the shape of the girder can be determined. Parameters are given in Tab. 3. Mass and inertial mass are $5.241\mathrm{kg/m}$ and $0.11\mathrm{kg \cdot m^2/m}$, respectively. Frequencies of heaving mode and pitching mode are $2.055\mathrm{Hz}$ and $5.429\mathrm{Hz}$, respectively.

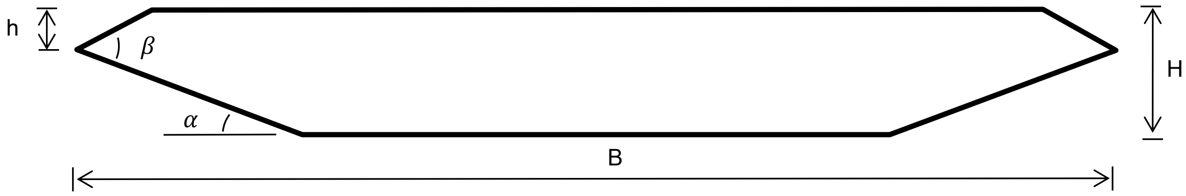

Fig. 7 Control effects with different slotting widths. (a) Tendencies of flutter critical speed. (b) Tendencies of growth rate.

Tab. 3 Shape parameters in case settings (m).

β	parameters	α					
		10	12	14	16	18	20
50	B	0.548	0.543	0.537	0.531	0.524	0.517
	h	0.025	0.021	0.018	0.014	0.011	0.008
60	B	0.533	0.530	0.526	0.521	0.516	0.511
	h	0.026	0.023	0.019	0.016	0.012	0.009

Tab. 4 Flutter critical speed in each case.

α	$+3°$		$0°$		$-3°$	
	$\beta = 50°$	$\beta = 60°$	$\beta = 50°$	$\beta = 60°$	$\beta = 50°$	$\beta = 60°$
10	130.4	117.7	135.1	127.2	158.0	157.2
12	154.8	126.4	140.6	135.9	161.9	156.4
14	155.6	128.0	143.0	144.6	158.0	158.0
16	144.6	128.8	150.1	149.3	160.4	160.4
18	143.8	132.7	150.9	152.5	158.8	158.8
20	138.3	124.9	157.2	157.9	165.1	165.1

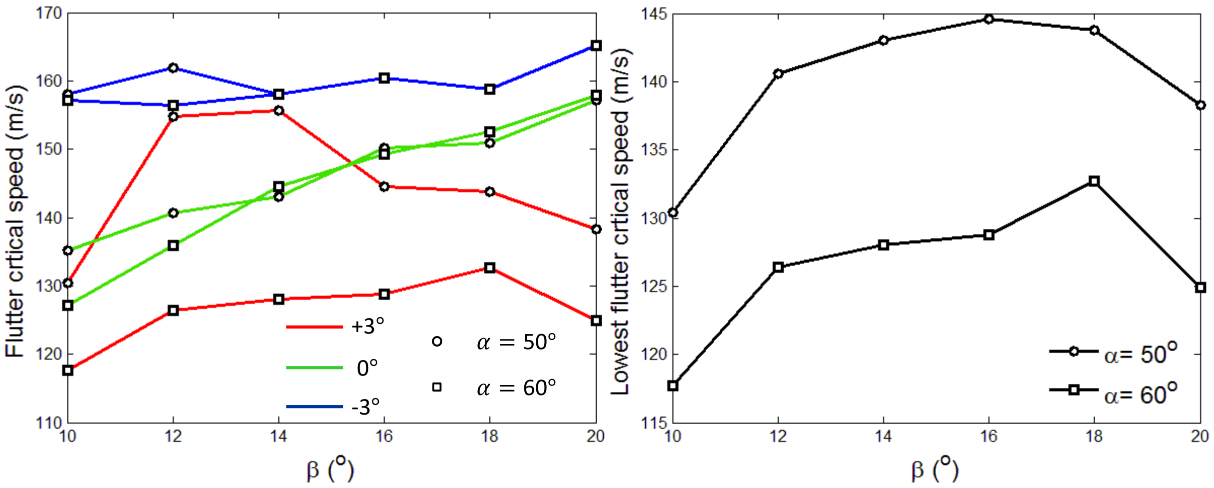

Fig. 8 Control effects. (a) Flutter critical speeds. (b) The decisive critical speeds.

The results of the critical speeds are given in Fig. 8. It can be recognized that the decisive critical speed increases firstly and then drops, when the dip angle α of the inclined web increases. And, smaller faring angle always means higher flutter stability. Actually, a much more simple conclusion can be described as: shaper fairings are better for flutter control.

3. SUGGESTED FACILITIES FOR BLUFF GIRDER WITH CANTILEVER

Cantilevered bridge girder is widely used in middle-span bridges. Its aerodynamic behaviors are normally worse than streamlined box girder. However, it's more economical because composite beam technique can be easily introduced, using concrete upper flange and steel lower flange and webs.

A series of wind tunnel tests are carried out, based on the East China Sea Bridge, which has a main span of 420m. Dimensions of the main girder's cross section are given as Fig. 9. As slotting is only useful when the original deck's flutter stability is good, its control effect is limited in such kind of a bluff body. However, it is found that stabilizer is still a good choice. And moreover, positions of the inspection rails can be adjusted, resulting different flutter stability.

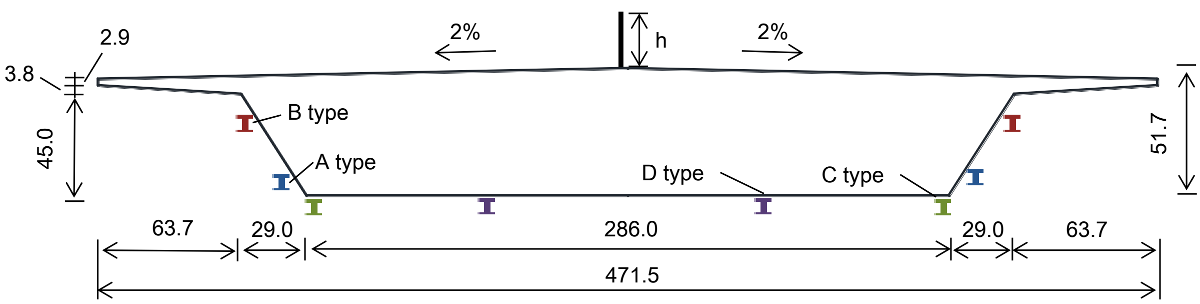

Fig. 9 Demonstration of the stabilizer and different types of inspection rails (mm).

The height of the central stabilizer and the types of the inspection rails are demonstrated in Fig. 9, down scaled with ratio of 1:70. Different cases are analyzed with constant dynamic characteristics. Mass and inertial mass are $54.47\mathrm{t/m}$ and $4224\mathrm{t\cdot m^2/m}$, respectively. Frequencies of heaving mode and pitching mode are $0.3578\mathrm{Hz}$ and $0.5897\mathrm{Hz}$, respectively.

3.1 stabilizer

Similar to the control effects in streamlined box girder, the stabilizer is more helpful when installed on the upper flange. The height of the stabilizer is adjusted as 20%, 25% and 30% of the deck height, respectively. The resulted flutter critical speed is given in Tab. 5. As shown in Tab. 5, central stabilizer with 25% of the deck height work best. The decisive critical speed is increased by 11%.

Tab. 5 Flutter critical speed with changing stabilizer height.

Wind attack angle	Original	$h = 20\%H$	$h = 25\%H$	$h = 30\%H$
$-3°$	>176.0	>176.0	>176.0	>176.0
$0°$	145.0	151.8	151.8	154.0
$+3°$	81.4	85.8	85.8	90.2

3.2 inspection rails

Inspection rails are used to examine and repair the steel part of the cantilevered box. Wind tunnel tests have shown that their positions can influent the girder's aerodynamic behavior. Therefore, several positions of the rails are studied to find out one with highest flutter stability. In each cases, the stabilizer with 25% deck height is also installed. The results are shown in Tab. 6. When the inspection rails are installed at the bottom of the inclined webs, the flutter stability is significantly improved, much higher than traditional position at the bottom of the lower flange.

Tab. 6 Flutter critical speed with changing rails position.

Wind attack angle	Original	Type A	Type B	Type C	Type D
$-3°$	>176.0	>176.0	>176.0	>176.0	> 176.0
$0°$	145.0	162.8	151.8	121.0	154.0
$+3°$	81.4	94.6	88.0	79.2	90.2

4. SUGGESTED FACILITIES FOR Π SHAPED GIRDER

Π shaped girder is an another widely used girder type for cable supported bridges. Its torsional stiffness is much weaker than box girder, and the aerodynamic characters are also worse. However, the concrete upper flanges make this girder type much cheaper. For this reason, it is used in lots of cable stayed bridges, like the 602m main span Yangpu Bridge, the 605 main span Qingzhou-Minjiang Bridge.

4.1 stabilizer

Previous studies have found that the turbulences generated at the bottom space of the Π shaped girder are critical for its flutter stability (Zhou, 2009). Two type of the stabilizer are therefore installed below the deck flange, to suppress the formation of large turbulence bubbles. The shape of the studied girder is given in Fig. 10. One type is traditional central placed stabilizer, the other type is off-center placed stabilizer. The latter one is to maximize the suppression effect for the flow in the bottom space.

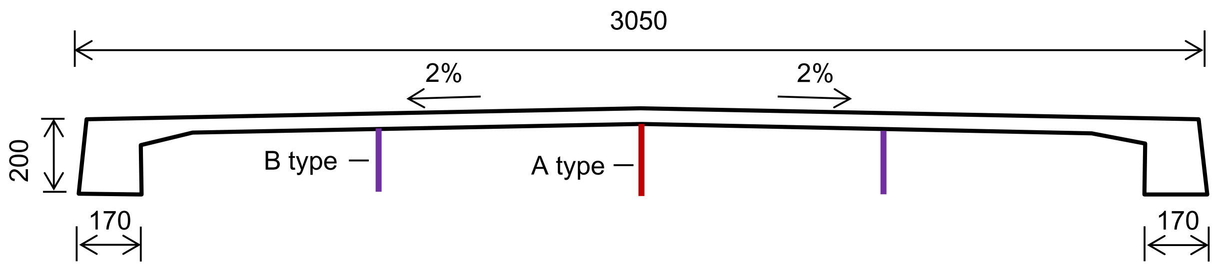

Fig. 10 Girder shape and the locations of two stabilizer types (cm).

The results of the wind tunnel tests have verified the intention of the stabilizers. Compared to the 62m/s flutter critical speed of the original shape, the 86m/s critical speed of the adjusted shape with Type A stabilizer is highlighted. Moreover, when the Type B stabilizer is installed, the critical speed is furtherly increased to 123m/s, making the flutter stability almost two times of the original one.

4.2 wind faring

Wind fairings are commonly effective for flutter control of bluff bodies. For such Π shaped bridge girder, they can suppress the flow separation at the corners of the two boxes, shown in Fig. 11. While the original flutter critical speed is 72.5m/s, it is raised to 95m/s when the wind fairings are installed.

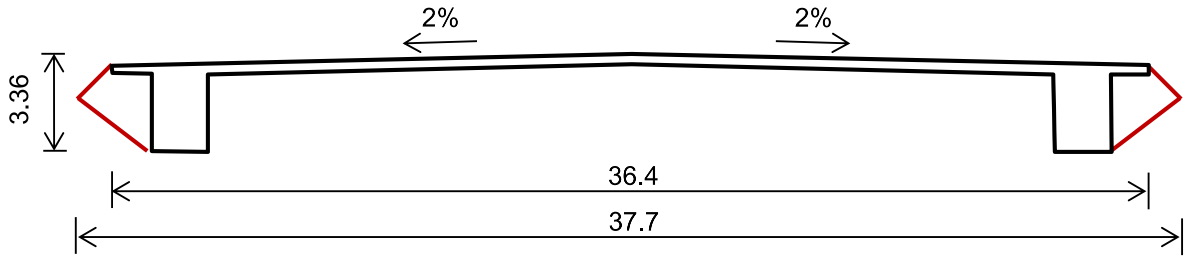

Fig. 11 Girder shape and the locations of two stabilizer types (m).

5. CONTROL MECHANISM INVESTIGATION

To investigate mechanisms of the passive aerodynamic facilities, CFD method is utilized to give an intuitive comparison of the flow between the cases with and without control. In previous studies, RMS of the pressure amplitude are commonly focused on. However, this is only one factor which affect the flutter stability. The reason is simple:

Firstly, the changing surface pressure covers a wide frequency range, in which only the component with the same frequency to the flutter oscillation contributes most to the stability. RMS value which reflects the whole frequency domain is ambiguous. Secondly, phase information is lacking if only RMS value is considered. The flutter instability occurs when the aerodynamic force is almost in-phase of the girder vibration. Otherwise, the aerodynamic forces will hinder the divergent oscillation, by doing negative work.

For these two reasons, the mechanism investigation followed are carried out based on the steps described below:

a) Obtaining flutter derivatives of the deck with and without certain passive facility.
b) Evaluating the flutter critical speeds, given the dynamic characters of the bridge structure.
c) Choosing one wind speed point U_m between the two critical speeds of the original deck and the one with control.
d) Verification of the chosen speed, by simulating the time-history of the two decks.
e) Extracting the oscillation information of the original deck, like the phase between the heaving and pitching mode, the amplitudes.
f) Diving the two decks vibrate in the same way, using the oscillation pattern extracted in step e). This is to make the aerodynamic shape the only changed factor.
g) Filtering the flow field to eliminate the less important high frequency components, to make the fluctuation with the flutter frequency clear.
h) Calculating the phase-averaging work of the surface pressure, to highlight the details of the total effect of the changed amplitude and phase.
i) It can be found that the integrated total work will be positive in the original case, but negative in the controlled case. It implies that the passive facility will change the instability of the deck in this given wind speed $\mathrm{U_m}$, if free-vibration condition is applied.

5.1 stabilizer

According to the schedule mentioned above, flutter derivatives are firstly obtained. With the dynamic characteristics of the GBB bridge, flutter critical speed is found to be 74m/s for the original section, and 84m/s for the improved section (with 20%D height central stabilizer). The checking wind speed U_m is chosen as 80m/s, where the original deck section become instable. Vertical and torsional displacements are given in Fig. 12.

Fig. 13 gives one time cycle of the filtered flow field. It can be recognized that the change of the pressure mostly happens above the upper flange. Firstly, the field oscillation in the windward zone is suppressed. Secondly, an additional negative pressure zone appears behind the stabilizer.

Fig. 14 gives the phase-averaged work of the surface pressure. It is obvious that the windward part of the upper flange and the lower flange changes little, when the stabilizer is installed. However, the positive work zone (which implies contribution of instability) located at the leeward upper flange is replaced by a negative work zone.

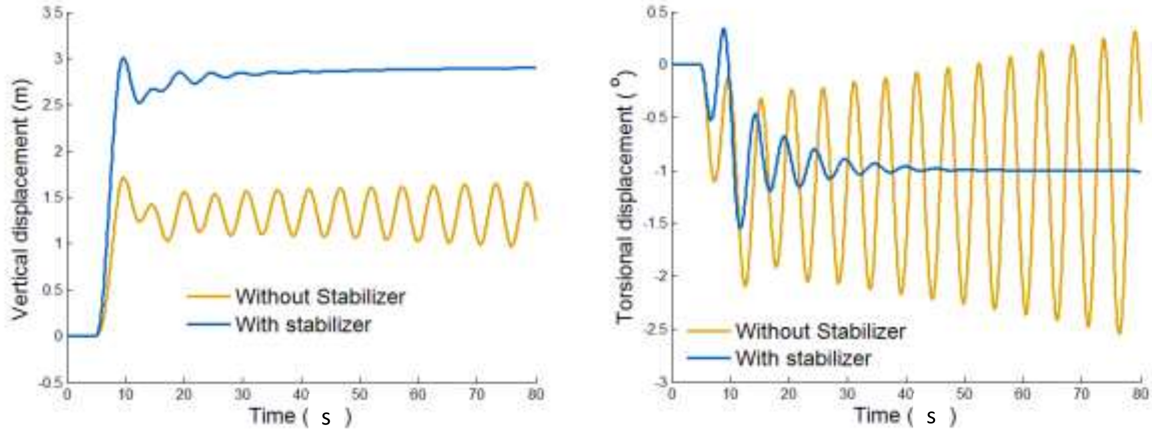

Fig. 12 Vibration comparison between the deck section with and without stabilizer.

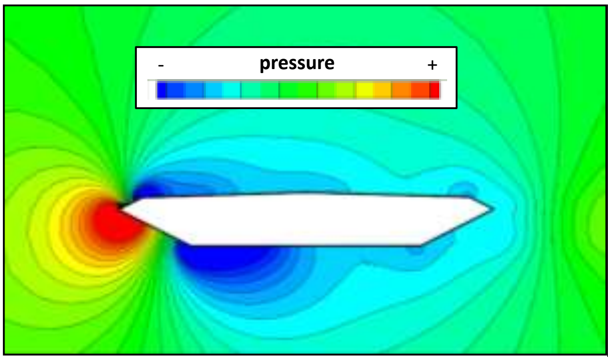

(a) $Time = 1/4\ cycle\ time$

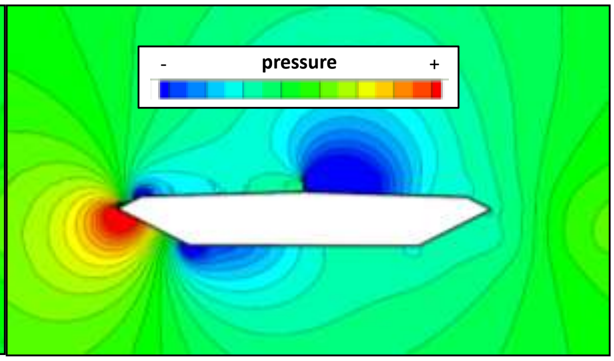

(e) $Time = 1/4\ cycle\ time$

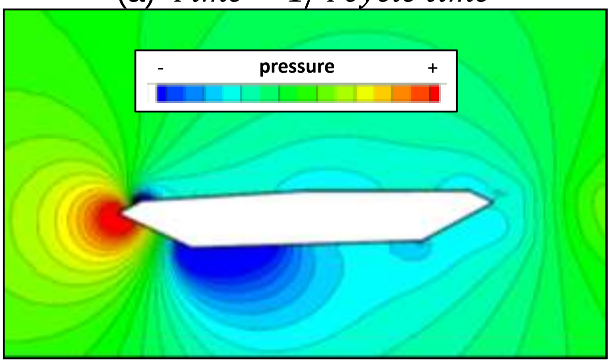

(b) $Time = 2/4\ cycle\ time$

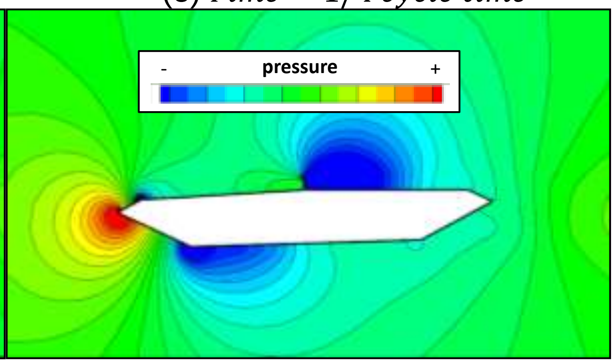

(f) $Time = 2/4\ cycle\ time$

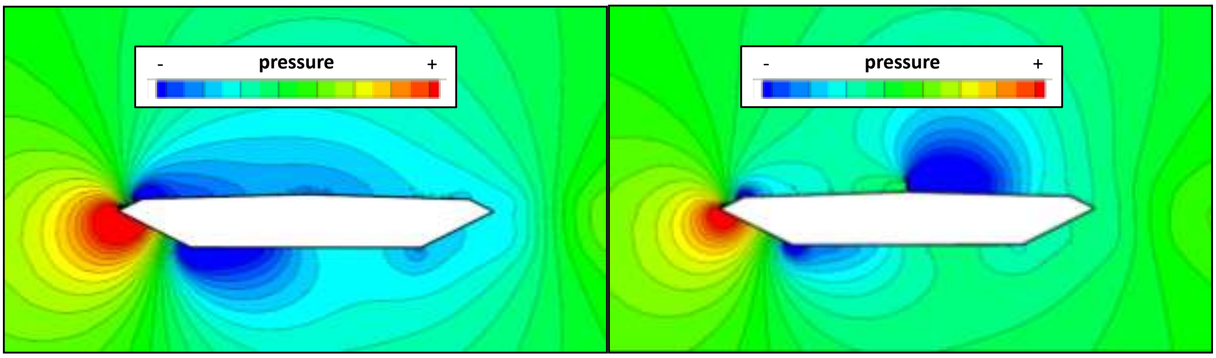

(c) $Time = 3/4\ cycle\ time$ (g) $Time = 3/4\ cycle\ time$

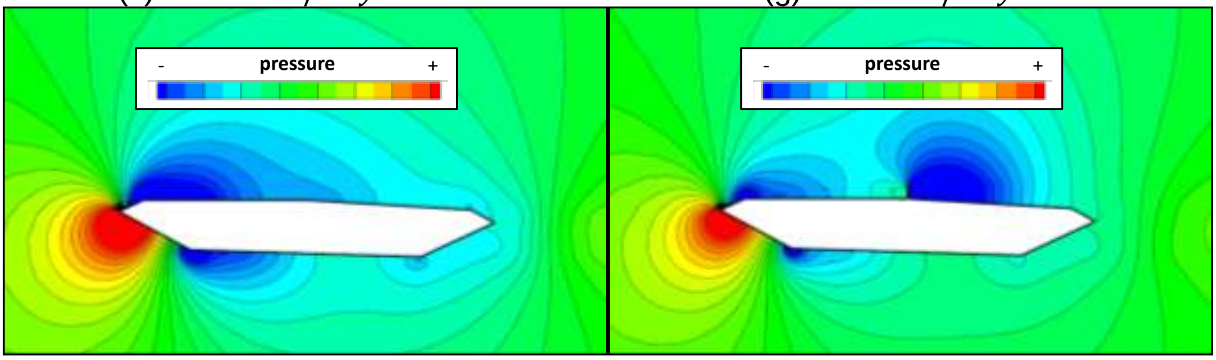

(d) $Time = 4/4\ cycle\ time$ (h) $Time = 4/4\ cycle\ time$

Fig. 13 Comparison of the filtered flow field. (a-d) with stabilizer. (e-f) without stabilizer.

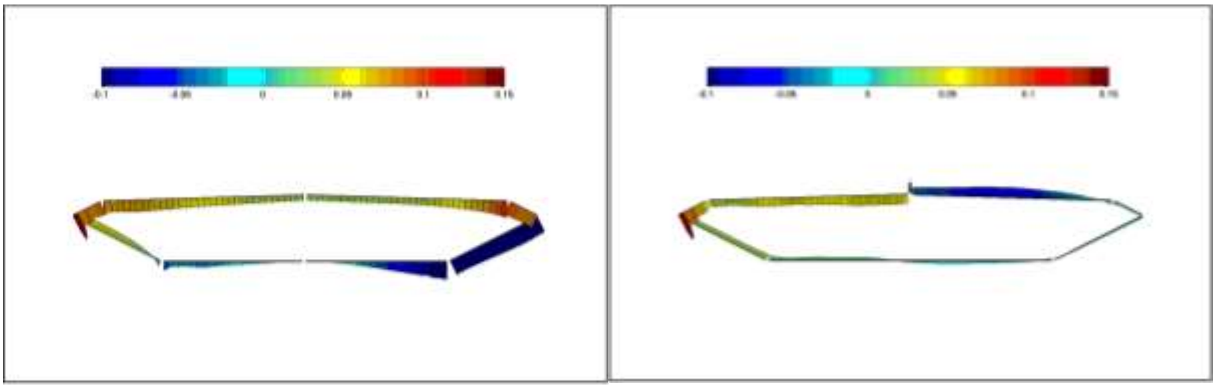

Fig. 14 Comparison of the phase-averaged work of the surface pressure (with and without stabilizer).

5.2 inspection rails

Similarly, flutter derivatives are firstly obtained. With the dynamic characteristics of the East China Sea Bridge, flutter critical speed is found to be 96m/s for the original section, and 146m/s for the improved section (with adjusted rail position). The checking wind speed U_m is chosen as 110m/s, where the original deck section become instable. Vertical and torsional displacements are given in Fig. 15.

Fig. 16 gives one time cycle of the filtered flow field. It can be recognized that the change of the pressure mostly happens below the lower flange. The amplitude of the field oscillation is suppressed.

Fig. 17 gives the phase-averaged work of the surface pressure. Rather than the highlighted field change in Fig. 16, It reveal additional information about the pressure under the cantilever. It is obvious that the pressure work of the windward-upper zone and leeward-lower zone of the cantilevers are changed from positive to negative, when the position of the inspection rail is adjusted to the bottom of the inclined web. The total work of the aerodynamic force is found to become negative after this optimization.

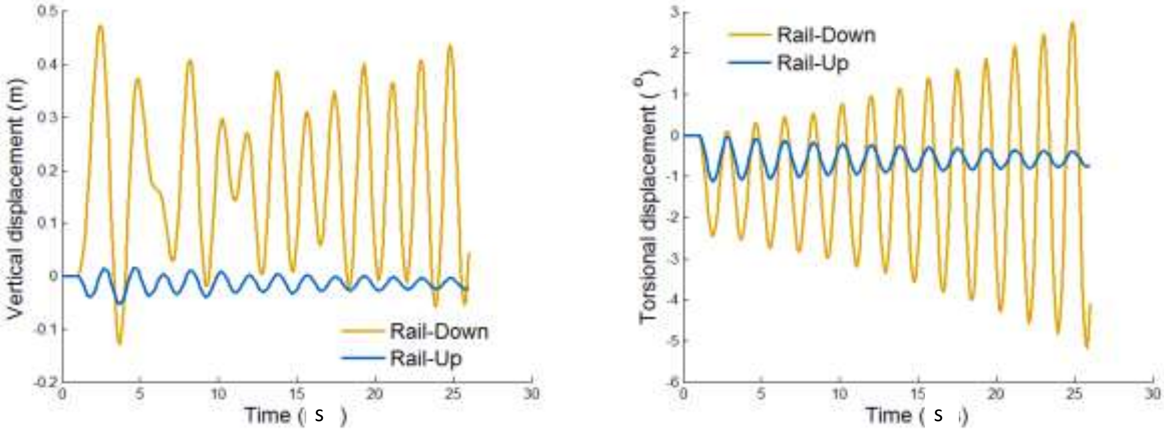

Fig. 15 Vibration comparison between the deck section with different rail position.

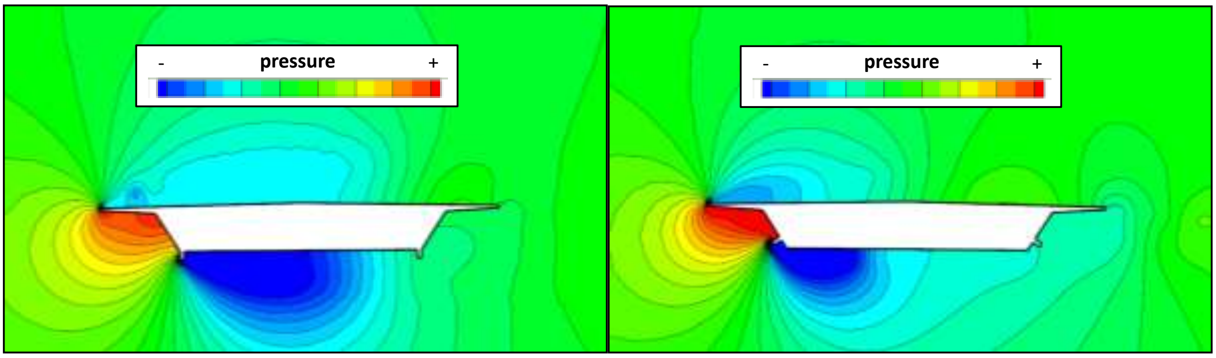

(a) $Time = 1/4\ cycle\ time$ (e) $Time = 1/4\ cycle\ time$

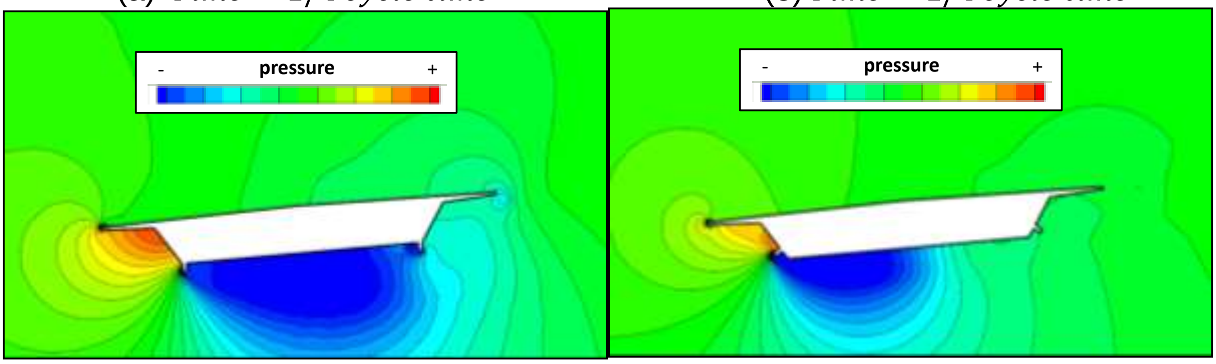

(b) $Time = 2/4\ cycle\ time$ (f) $Time = 2/4\ cycle\ time$

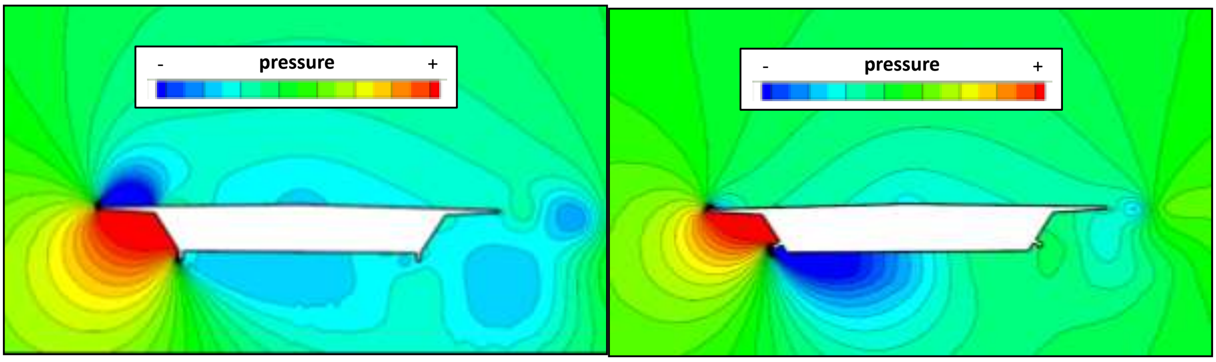

(c) $Time = 3/4\ cycle\ time$ (g) $Time = 3/4\ cycle\ time$

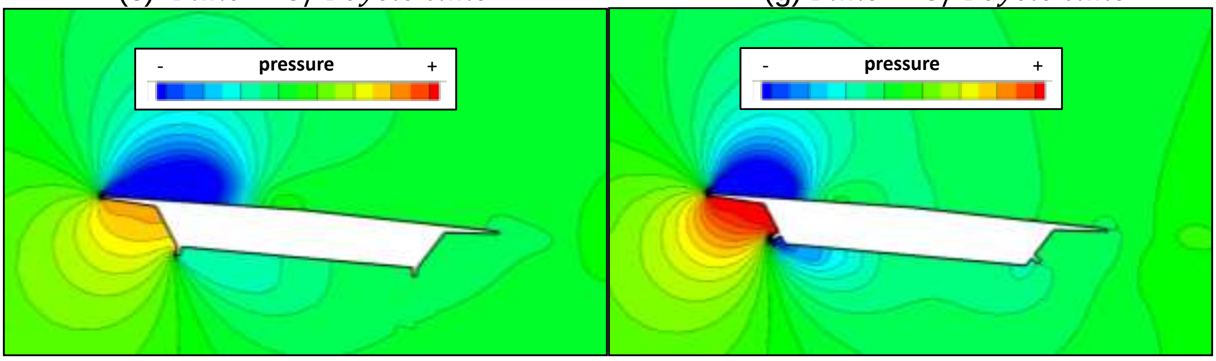

(d) $Time = 4/4\ cycle\ time$ (h) $Time = 4/4\ cycle\ time$

Fig. 16 Comparison of the filtered flow field. (a-d) with lower rail. (e-f) without upper rail.

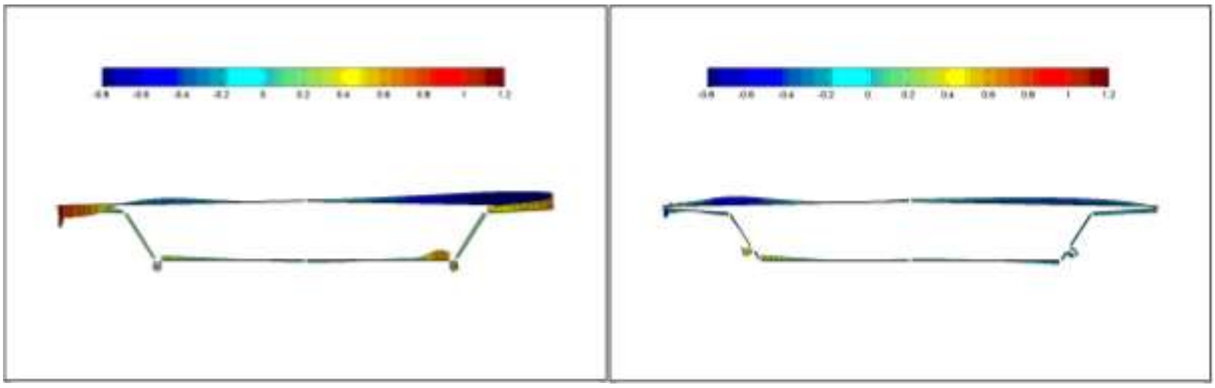

Fig. 17 Comparison of the phase-averaged work of the surface pressure (different rail position).

5.3 wind faring

According to the same schedule, flutter derivatives are firstly obtained. With the dynamic characteristics of a cable-stayed bridge under construction, flutter critical speed is found to be 106m/s for the original section, and 130m/s for the improved section (with wind faring). The checking wind speed U_m is chosen as 110m/s, where the original deck section become instable. Vertical and torsional displacements are given in Fig. 18.

Fig. 19 gives one time cycle of the filtered flow field. It can be recognized that the change of the pressure mostly happens in the lower space, surrounded by the two boxes and the upper flange. An additional positive pressure zone appears in the leewrd direction.

Fig. 20 gives the phase-averaged work of the surface pressure. It shows that the positive work, which locates in the leeward part bellow the flange, is suppressed. Moreover, the negative work, which locates at the lower surface of the leeward box, is augmented. The overall work has become negative, after the installation of the wind faring.

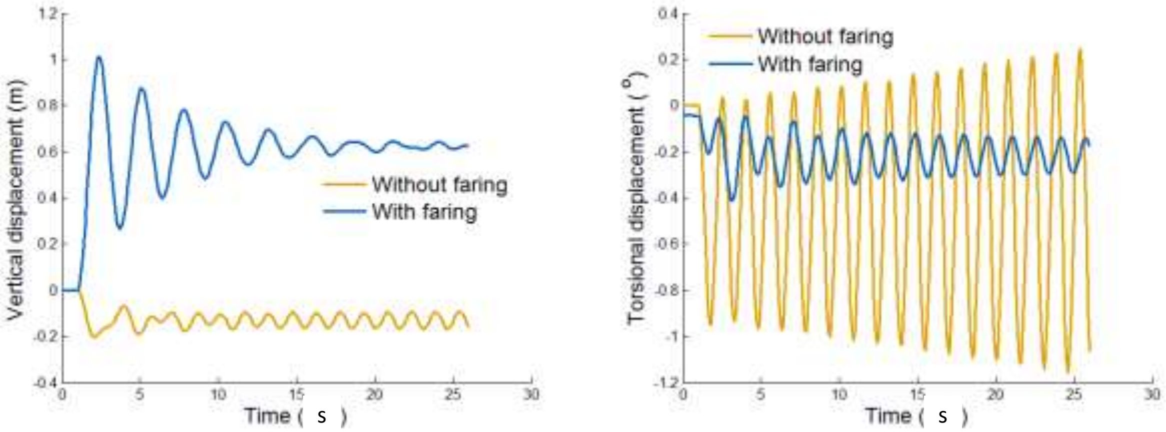

Fig. 18 Vibration comparison between the deck section with different rail position.

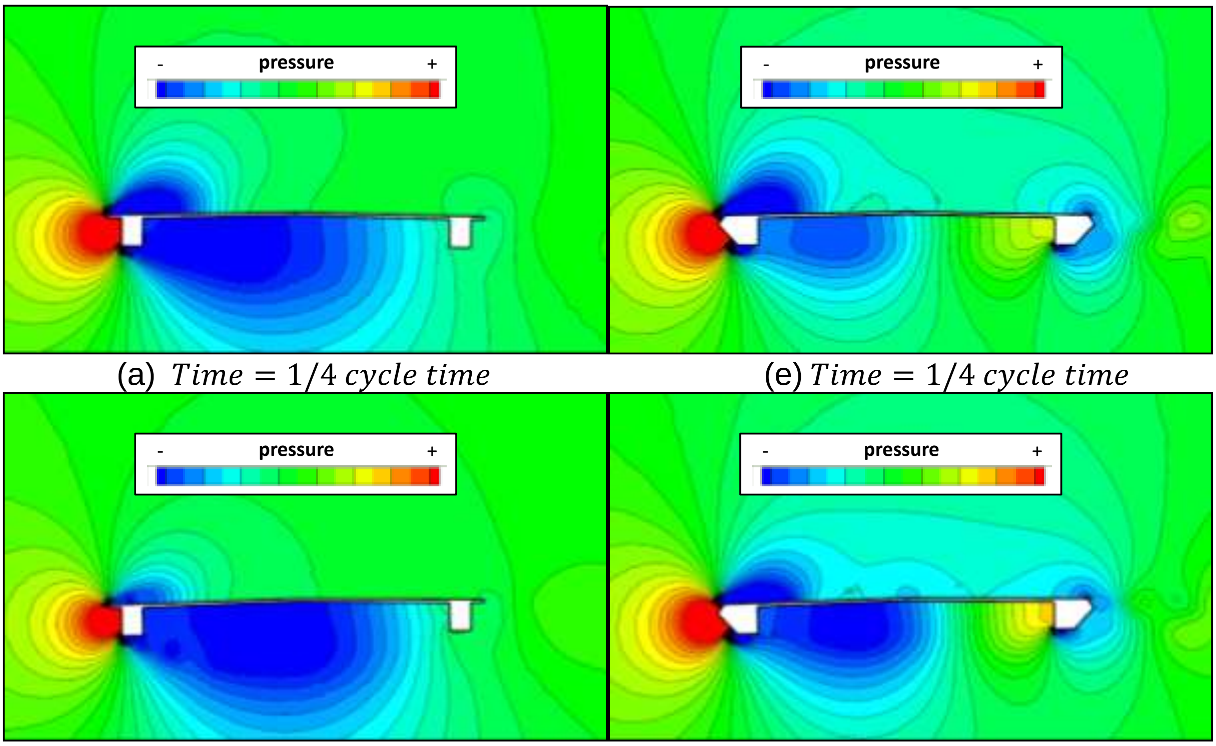

(a) $Time = 1/4\ cycle\ time$ (e) $Time = 1/4\ cycle\ time$

(b) $Time = 2/4\ cycle\ time$ (f) $Time = 2/4\ cycle\ time$

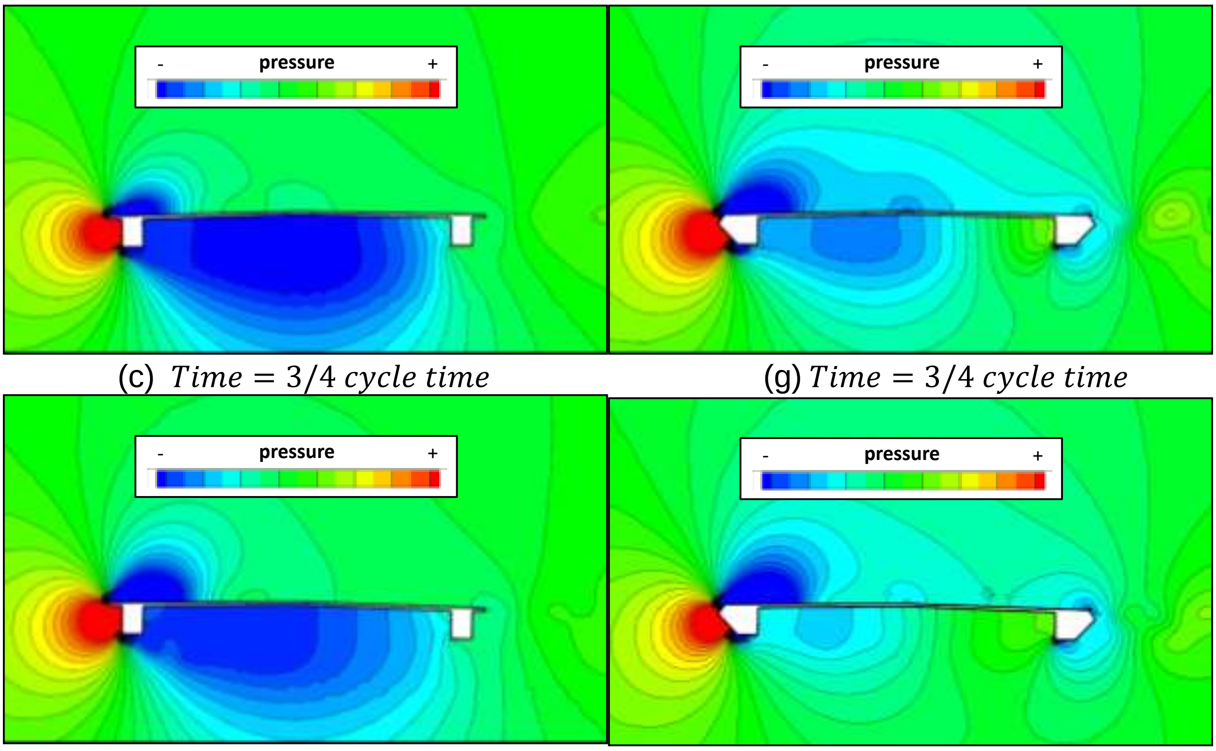

(c) $Time = 3/4\ cycle\ time$ (g) $Time = 3/4\ cycle\ time$

(d) $Time = 4/4\ cycle\ time$ (h) $Time = 4/4\ cycle\ time$

Fig. 19 Comparison of the filtered flow field. (a-d) without faring. (e-f) with faring.

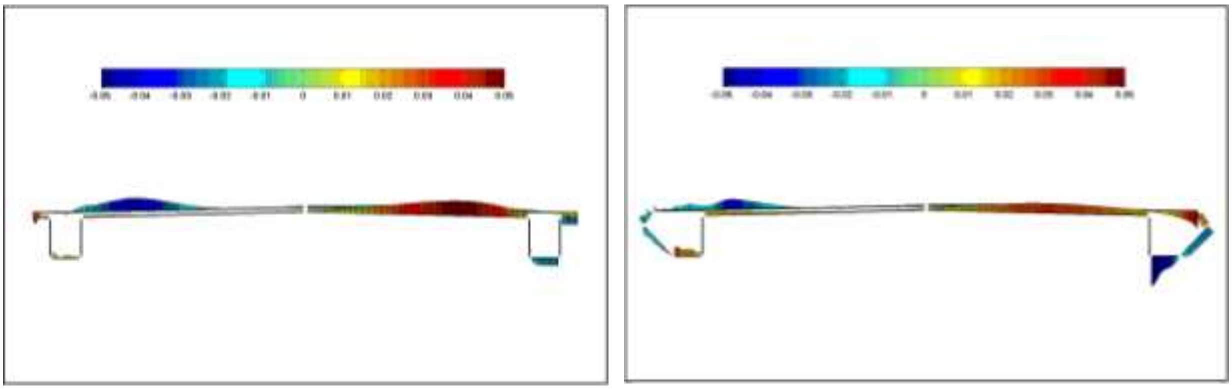

Fig. 20 Comparison of the phase-averaged work of the surface pressure.

6. CONCLUSIONS

Slotting, stabilizer, inspection rails and wind faring are studied as passive control facilities for aerodynamic flutter of bridge girder. Their control effects are found to be obvious in particular girder types. For this reason, their parameter sensitivity, control robustness and mechanisms for streamlined box girder, Π shaped girder and cantilevered girder are studied through wind tunnel tests and CFD method, aiming to give some inspiration of future researches.

REFERENCES

Billah, K.Y. and Scanlan, R.H (1991), “Resonance, Tacoma Narrows Bridge failure, and undergraduate physics textbooks”, the American Journal of Physics, 59(2):118-124.

Brown, W.C. (1996), “Development of the deck for the 3300m span Messina”, 15th IABSE Congr. Rep., 1019-1030.

Ge, Y.J. and Xiang, H. F. (2011), “Extension of bridging capacity of cable-supported bridges using double main spans or twin parallel decks solutions”, Structure and Infrastructure Engineering: Maintenance, Management, Life-Cycle Design and Performance, 7(7-8):551-567.

Makoto K. (2004), “Techonology of the Akashi Kaikyo Bridge”, Structural Control and Health Monitoring, 11:75-90.

Miyata, T. (2003), “Historical review of long-span bridge aerodynamics”, Journal of Wind Engineering and Industrial Aerodynamics, 91:1393-1410.

Simiu, E., and Scanlan, R. (1986), “Wind effects on structrues”. John Wiley & Sons, Inc., New York, N.Y.

Wang D.Z. (2010), “Geometrical optimization of closed box girders based on aerodynamic performance”, Master Thesis. Tongji University.

Yang Y.X., Zhou R., Ge Y.J. (2014), “Practical flutter control method for long-span bridges”, Journal of Tongji University (Natural Science), 42(7):889:997.

Zhou X.J. (2005), “Study on the flutter control facilities and their mechanisms for long-span suspension bridges”, Master Thesis. Tongji University.

Zhou Z.Y., Yang L.K. (2009), “On the mechanism of vertical stabilizer plates for improving aerodynamic stability of bridges”, Acta Aerodynamica Sinica, 27(6):683-689.